

Ing. Lucie DOBIÁŠOVÁ
Ing. Daniel ADAMOVSÝ, Ph.D.

CTU in Prague, Faculty of Civil
Engineering, Department of
Indoor Environmental and
Building Services Engineering

Reviewer
Ing. Petr ZELENSKÝ

The CFD Simulation of a Standing Person in an Indoor Environment

CFD simulace stojícího člověka ve vnitřním prostředí

The article presents a virtual model of a standing person in an indoor environment. A virtual manikin is placed in the room with displacement ventilation where the cold air supplied to the room at low velocity is heated by heating sources and rises up due to buoyancy forces. The calculation is carried out for three different turbulence models: $k-\omega$ SST, $k-\epsilon$ Realizable and $k-\epsilon$ RNG. The simulation results are compared with experimental data using velocity and temperature profiles in four transverse planes. As a result, the verified model of a person is obtained that can further be applied to the particular conditions.

Keywords: CFD, indoor environment, heat sources, occupants, convective flow, numerical model, turbulence model

Článek představuje virtuální model stojící člověka ve vnitřním prostředí. Virtuální manekýn je umístěn do prostoru se zaplavovacím větráním, kdy je do místnosti přiváděn chladný vzduch nízkou rychlostí, který je ohříván od tepelných zdrojů a díky vztlačovým silám stoupá vzhůru. Výpočet je proveden pro tři různé modely turbulence – $k-\omega$ SST, $k-\epsilon$ Realizable a $k-\epsilon$ RNG. Výsledky simulace s experimentálními daty jsou porovnány pomocí rychlostních a teplotních profilů ve čtyřech příčných rovinách. Výsledkem je ověřený model člověka, který lze dále aplikovat do konkrétních podmínek.

Klíčová slova: CFD, vnitřní prostředí, zdroje tepla, konvektivní proud, numerický model, model turbulence.

INTRODUCTION

According to ASHRAE Guidelines [1], people spend 80–90 % of their time in buildings. It is proven that problems with indoor environment quality (IEQ) directly influence the comfort, health and productivity of the people [2, 3]. The indoor environment and its quality can be assessed by a couple of factors such as the thermal comfort, the air quality, the mental comfort, the acoustic comfort, etc. All the aforementioned parts create a set that may have both a short-term and long-term impact on the individuals [4, 5].

There are pollutants of various compositions and in various quantities in the indoor environment. A part of these pollutants enters the building from the outdoor environment due to the ventilation air, while others can be produced directly in the building. Typical sources include building materials and internal equipment such as computers, printers, etc. However, man himself and his activities represent the greatest sources of pollutants in the indoor environment. A person in the indoor environment functions as an obstacle for air flow in the room, is a significant heat source inducing convective flow and, last but not least, a source of carbon dioxide, odours, and microbes.

In recent years, the issue of the possible transfer of pollutants among individuals has come to the forefront. This topic was subject to several experimental studies [6, 7] that have examined the influence of both the distance and position between two people. Such experiments require two or more thermal manikins and the necessary laboratory apparatus, whose purchase price is rather high. As an alternative, a Computation Fluid Dynamics (CFD) simulation with a model comprising one or more people can be used. Thanks to numerical modelling, it is possible to obtain a general picture of the room's airflow and of the temperature field distribution, particularly in the vicinity of the human body. To examine the quality of the inhaled air and the risk of pollutants spreading, advanced models with a breathing function added can be used, for more info, refer to works of Bjorn and Nielsen [8] or Gao and Niu [9].

A disadvantage of the computer model (in addition to the required computational resources and time) is the necessity of having the results verified, preferably using measured data obtained by experimentation. Since it is neither possible nor effective to solve each task experimentally, the model can be validated on the basis of a similar task or using benchmark tests. The latter represent a set of boundary conditions and the resulting data of the required quantities that can be used for the verification of the task. For the purposes of this study, the benchmark test made by Nielsen in 2003 [10] has been used; the test will be described in detail in the following sections.

THE CFD MODEL

Model geometry

Models of a virtual person started appearing in the nineties of the last century and prevaillingly featured simplified shapes, i.e., cuboids or cylinders [11, 12, 13]. The advancing development of computer technology allowed for the creation of more precise models and even detailed shapes of a real man. The most complex geometries were then created by laser scanning of thermal manikins. Both groups (simplified as well as detailed models) have both advantages and disadvantages. The main advantage of the simple geometry consists in smaller demands for computational resources; it is more appropriate when providing a general picture of the airflow in the space being examined. If, however, the vicinity of person is a matter of interest, for example, when solving the quality of inhaled air and the spread of the pollutants, real complex geometry needs to be considered.

The model geometry of a person used in this study has been provided by Prof. P. V. Nielsen and his colleague Mr L. Liu. This virtual manikin (see Figure 1) represents a standing woman approx. 1.65 m high. It was created by laser scanning of a virtual manikin to have been used for the aforementioned benchmark test. The virtual manikin is divided into several segments, is naked and without hair. Both hands and feet are

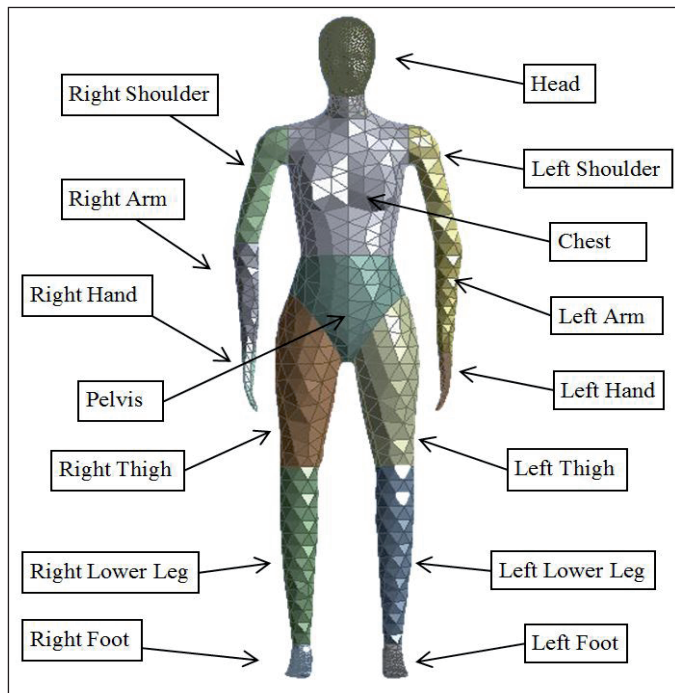


Fig. 1 Geometry of the virtual manikin

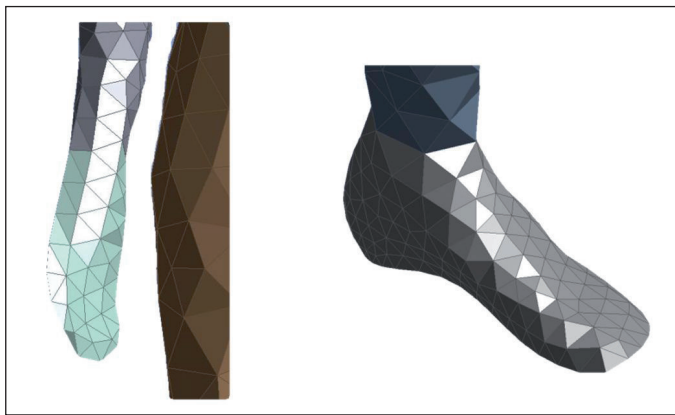


Fig. 2 Simplification of the hands and feet

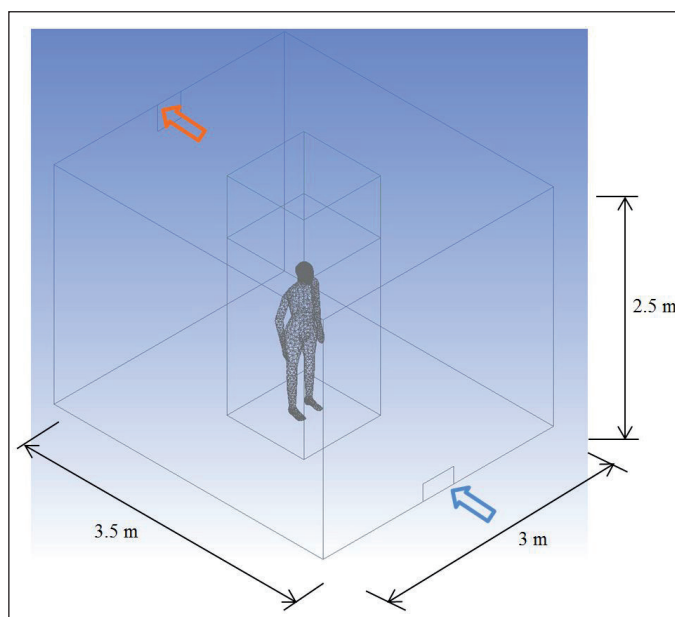


Fig. 3 Diagram of the chamber

simplified (see Figure 2) because they are not critical for the picture of the airflow in the surroundings of the body. The total area of the body is 1.48 sq. meters.

Figure 3 shows the geometry of the solved area corresponding to the experimental chamber in which the benchmark test was made. It is a space that has the dimensions of $3.5 \times 3 \times 2.5$ m and is equipped with a displacement ventilation system. In general, this system can be described as a system supplying cold air to the lower part of the room where indoor heat sources cause the air being heated to rise so that it carries away the pollutants. In this case the clean air enters the room via the inlet element near the floor that has the dimensions of 0.2×0.4 m and is located in the front wall in front of the manikin. An outlet with the dimension of 0.3×0.3 m is located in the rear wall under the ceiling. The manikin is placed in the middle of the room, 5 cm above the floor to avoid any heat conduction from the manikin to the floor.

Boundary conditions

The basic interaction between the human body and the environment is the transfer of heat produced due to the body's metabolism depending on the physical level. A part of this heat is accumulated inside the body, but the prevailing part is released into the surroundings and represents heat losses of man. These losses can be divided into sensible (due to convection, radiation and conduction) and latent (due to sweating, breathing and diffusion of water vapour through the skin). Most numerical calculations only consider the sensible losses, since the modelling of latent losses is a rather difficult process and requires that a thermoregulation model of a human body to be deployed. For the purposes of this study, only the sensible heat losses due to convection and radiation have been taken into account.

For the solution of the heat transfer between the man and his surroundings, the numerical methods can apply to two types of boundary conditions, the body surface temperature or the surface heat flux. The values of the body surface temperature may range from 31°C to 34°C [14 – 17]. When the heat flux is used as a boundary condition, its value will differ depending on whether or not the radiation is considered in the calculation. If only the convection is included the heat flux, it is between 20 W/m^2 [18] and 25 W/m^2 [7]. When the radiation is considered in the calculation, the value of the heat flux is usually over 50 W/m^2 , e.g., Ito et al. considered 51.6 W/m^2 [19] or Villi and De Carli used 53.5 W/m^2 [20].

The benchmark test prescribes a total heat load of 38 W for the convection only and 76 W for the model with the radiation. The radiation has been considered in all the simulations, as it may have a considerable influence on the final results [13]. The thermal boundary condition for the manikin was set up as a constant heat flux of 51.4 W/m^2 (i.e., considering the surface body area 1.48 m^2 , the total heat flux was equal to 76 W). The emissivity of the manikin's surface was 0.95 and 0.9 for the walls. In addition, 10 W has been added for the chamber surfaces as the heat flux according to the heat balance calculation by Srebric et al. [21]. The parameters of the inlet air are defined by the temperature of 21.8°C and the constant velocity of 0.182 m/s (i.e., the room air exchange rate was approx. 1.9 h^{-1}).

Calculation and model validation

The accuracy of the simulation results depends on the quality of the computational grid, the creation of which takes the prevailing time of the whole simulation process. To ensure the effective creation of the grid, the solved domain was divided into three parts: a cuboid around the virtual manikin, a cuboid in the area above the head where significant convective flow is expected, and a third area in the remaining space. The unstructured mesh was used for the entire domain, but with

different cell sizes for each part. The grid element size was 0.025 m in the cuboid around the manikin (with a surface element size of 0.007 m); 0.03 m above his head and 0.035 in the rest of the domain. In order to solve the boundary layer, ten layers of prismatic cells with a growth rate of 1.2 were created near the manikin's surface and seven layers with the same growth rate near the chamber walls. The value of y^+ over the manikin's surface was less than one. The computational grid has approx. 5 million cells altogether.

The selection of a turbulence model represents an important part of the computation. In the field of indoor environment modelling, two-equation models $k-\epsilon$ and $k-\omega$ are the most frequently used. In addition to the selection of a suitable turbulence model, it is important to properly solve the convective boundary layer for solid surfaces. It can be ensured by the application of a wall function or by the integration of the governing equations through the whole boundary layer.

The calculation was carried out for two turbulence models from the group $k-\epsilon$, i.e., $k-\epsilon$ Realizable and $k-\epsilon$ RNG (Re-Normalisation Group). In both cases, no wall function was used, which means that the calculation was made across the entire boundary layer. As the third model, which is also frequently used for the indoor environment simulations, the $k-\omega$ SST (Shear Stress Transport) model was applied. The steady-state simulations have been carried out with the SIMPLE algorithm for the pressure-velocity coupling. For the solver control, the residual target was set to 10^{-4} (10^{-6} for the energy). The radiation flux was calculated using the Discrete ordinates model.

The used benchmark test provides the measured values of the airflow velocity and air temperature in four poles (L1, L2, L4, L5), at several levels, as well as some results of the Particle Image Velocimetry (PIV) measurements made near the body (L3, L6). The places of the measurements are shown in Figure 4. Using the measured and simulated values, it is possible to assess the vertical profiles of the air velocities and temperatures in the individual locations and compare one turbulence model to another.

DISCUSSION OF THE RESULTS

Temperature field

Figures 5 through 8 show the comparisons of the calculated vertical temperature profiles in the L1, L2, L4 and L5 poles to the experimental

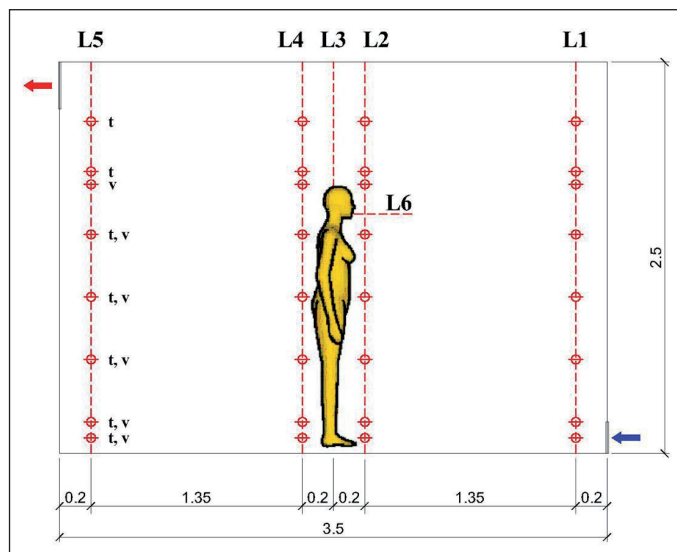


Fig. 4 Measurement locations (t – location for the air temperature measurement, v – location for the air velocity measurement)

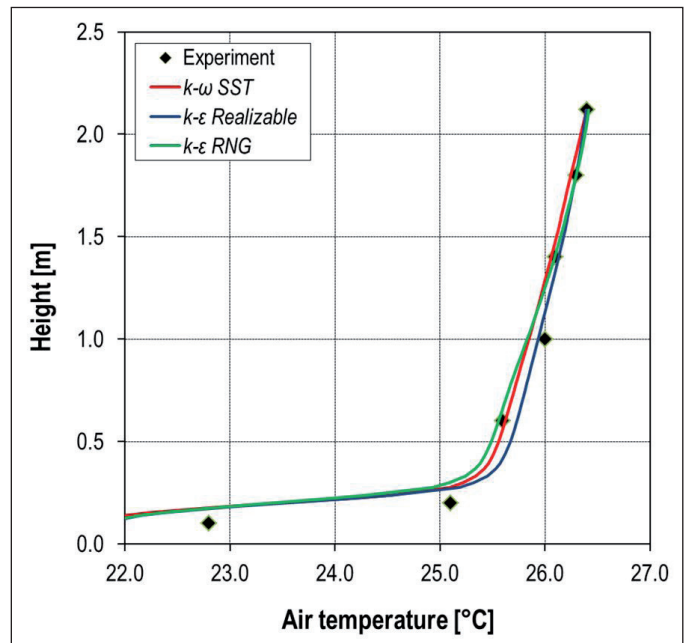


Fig. 5 Temperature magnitude profile (L1)

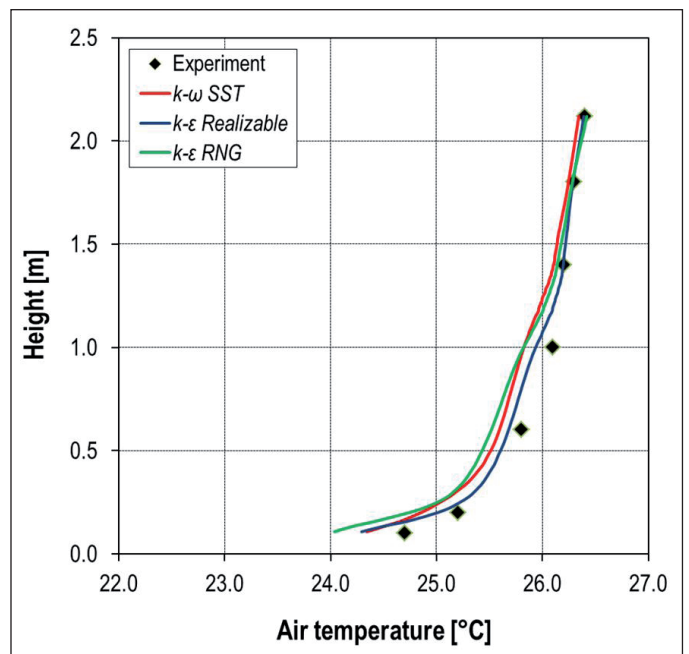


Fig. 6 Temperature magnitude profile (L2)

data. From the first comparison of the individual profiles, it is obvious that the turbulence models $k-\epsilon$ feature an almost identical course, while $k-\omega$ SST slightly differs, especially in L4. The models $k-\omega$ SST and $k-\epsilon$ Realizable at a level of 1 m show the greatest difference, nearly 0.5 °C. An interesting trend can be observed in the vertical profile, in position L5, where the differences in the individual cases at a level of 0.1 m are approx. 0.2 °C; with the increasing height, this difference gets smaller. In the highest point of the profile, the temperatures are practically identical.

In general, the trend of the results corresponds to the principle of the displacement ventilation when the air temperature shows the lowest value near the floor and starts increasing with the increasing height. Based on the diagrams, it is possible to read the total vertical temperature gradient in the room that shows the greatest value in L1, more than 4 °C. As

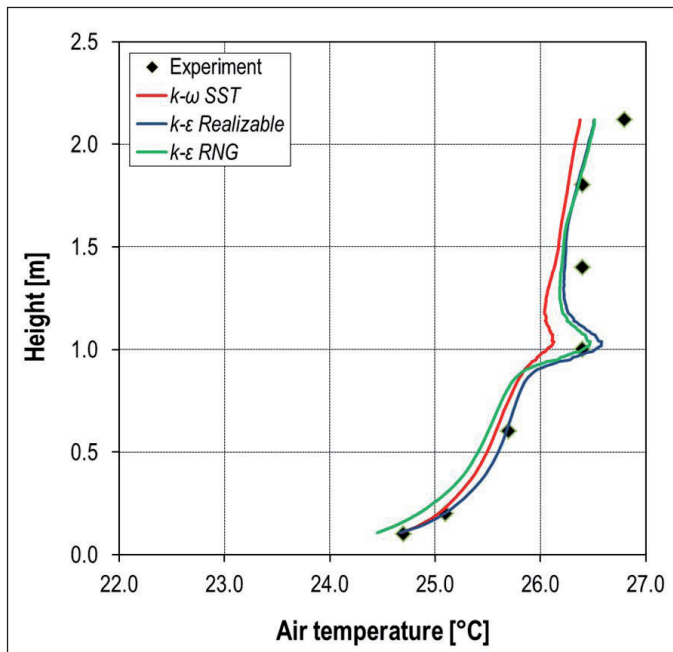


Fig. 7 Temperature magnitude profile (L4)

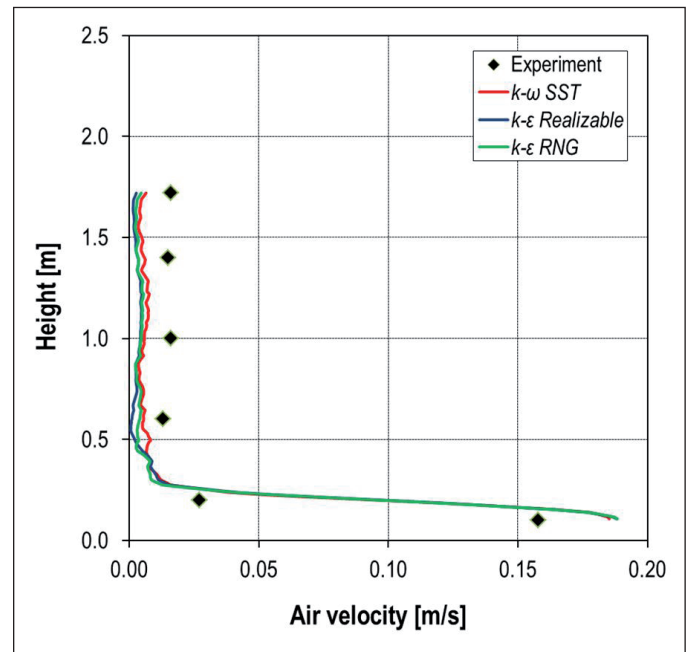


Fig. 9 Velocity magnitude profile (L1)

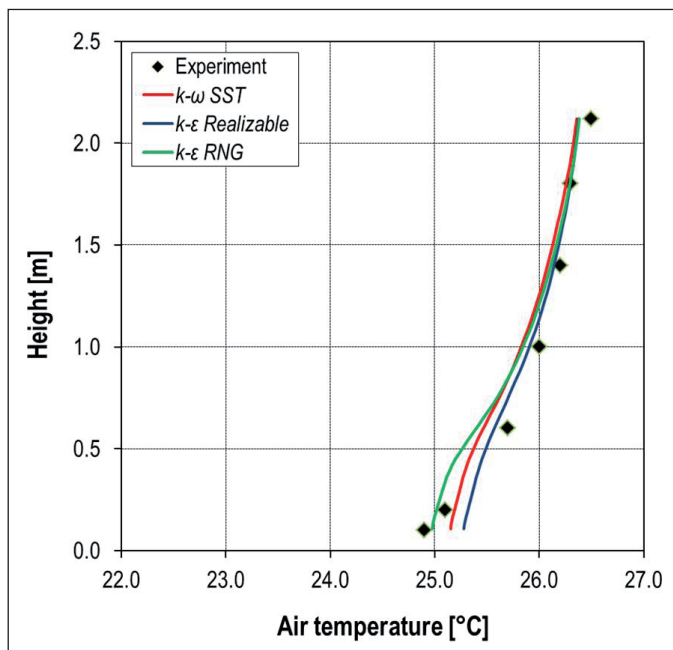


Fig. 8 Temperature magnitude profile (L5)

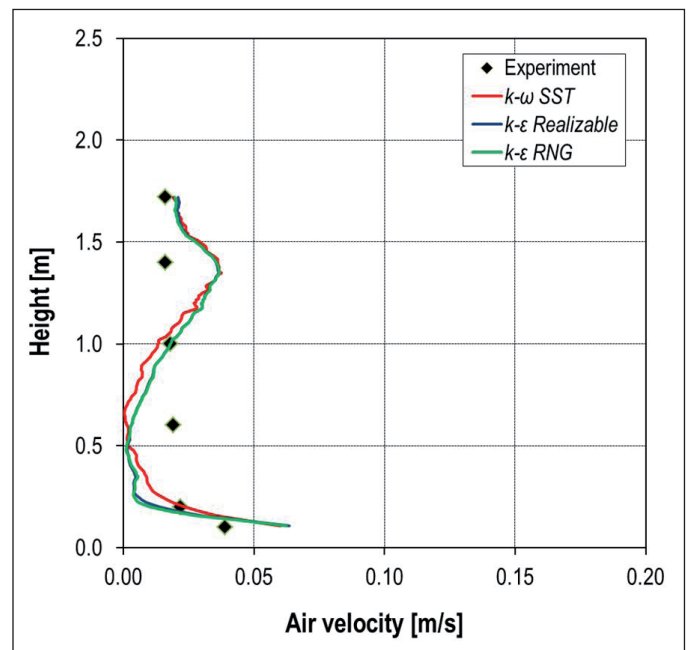


Fig. 10 Velocity magnitude profile (L2)

the air passes through the room, it slowly mixes with the heated air, and the temperature gradient gets lower in the other poles. In the location of the L2 profile and the L4 profile, it equals 2.5 °C and 2 °C, respectively; its lowest value, i.e., only 1.1 °C, was found in the last pole, L5.

Velocity fields

The following Figures (9 through 12) show the profiles of the airflow velocities. The velocity profiles in the simulations with the models $k-\epsilon$ are very similar to each other, while the $k-\omega$ SST slightly differs. The profiles in L1 and L5 show the smallest differences between the turbulence models; at the same time, these profiles show the same trend like the experimental data. Nevertheless, the calculated values in both profiles were lower when compared to the measured values. The reasons are not yet clear for this. One explanation can be the influence of the used turbulence model. Srebric et al. [21] reached

the same results with the $k-\epsilon$ models in both poles, as well as Deevy et al. [22] with $k-\omega$ SST, while the Large Eddy Simulation (LES) models slightly overestimated the air velocity in the study of Tagninia et al. [23]. The greatest differences between the individual models were found in L4 again, at the level of 1 m, where the $k-\epsilon$ models have significantly exceeded the $k-\omega$ SST model which corresponds to the experimental data very well. When the simulation results are compared to the experimental data, the greatest differences have been found in L4 as well as in L2, i.e., close to the manikin. In both profiles, the calculated velocities in the lower half of the chamber are lower when compared to the measured data, but from the level of 1 m upwards, they exceed the experimental data.

Summary of the results, and other model possibilities

To obtain a general view of the airflow in the space and the temperature

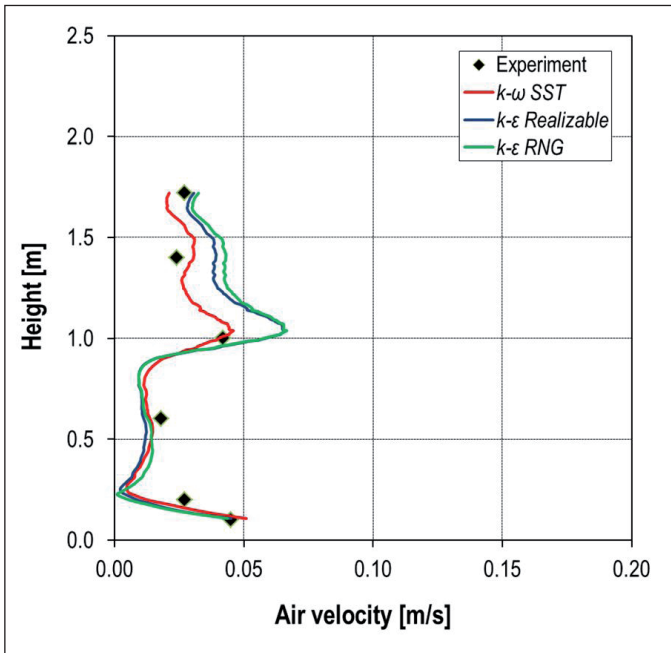


Fig. 11 Velocity magnitude profile (L4)

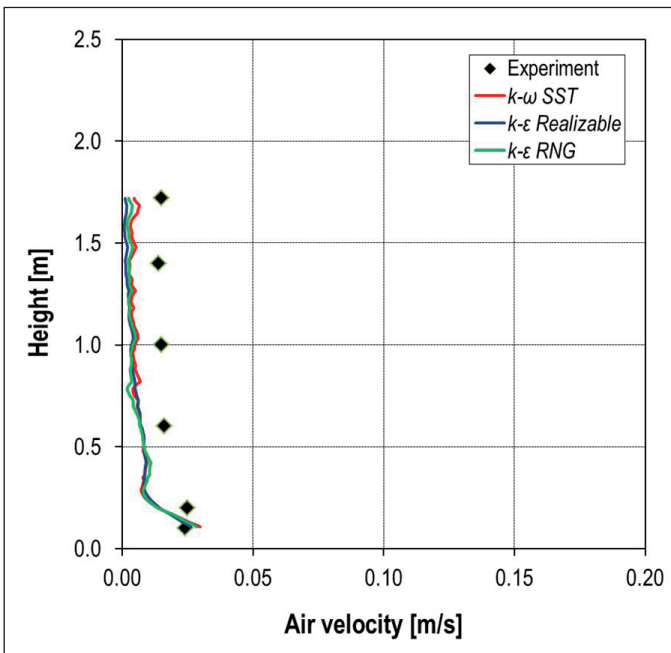


Fig. 12 Velocity magnitude profile (L5)

field distribution, Figures 13 and 14 show the longitudinal cross-sections through the middle of the room being solved. Both cross-sections illustrate the airflow from the inlet element in the front wall, the velocity of which becomes less with the increasing distance. Another significant flow that can be observed in the area around the virtual manikin is caused by the difference in the temperatures of the body surface and of the ambient air; it turns into a convective flow rising above the manikin's head. It is just this resulting buoyancy force that affects the exposure of man to air pollutants, especially when a displacement ventilation system is used [24, 25]. The rising heated air not only brings pollutants from the ambient air to the breathing zone, but also particles released from the human skin and clothing. Hence, it is obvious that the convective boundary layer around the human body imminently affects the occupants and has a high importance when solving the inhaled air quality, thermal comfort, etc.

CONCLUSION

The given article has presented a virtual model of an individual in the indoor environment. It is a woman approx. 1.65 m in height standing in the room equipped with a displacement ventilation system. The model geometry was created based on the benchmark test [10], to which the results have been compared. The calculation was made for three different turbulence models, *k-omega SST*, *k-epsilon Realizable* and *k-epsilon RNG* (in all the cases, no wall function was used). The simulation results were compared to the experimental data using the velocity and temperature profiles in four poles. The results of all the simulations corresponded to the trend of the experiments quite well; greater differences were found in the profile of the airflow velocities, particularly in the surroundings of the manikin. However, it should be noted that airflow velocities were very low in the entire space and did not exceed a value of 0.05 m/s except for the L4 profiles. At such low values, it is disputable as to what extent the measured data is relevant, because common anemometers are operated at an error up to ± 0.03 m/s. The individual turbulence models can also be compared in the area close to the manikin where the PIV measurements were made. Nevertheless, such an assessment is rather extensive and goes beyond the capacity of this article.

In conclusion, it is possible to say that the best compliance with the experiment was achieved in the turbulence model *k-epsilon Realizable*, namely in all temperature profiles. The *k-epsilon RNG* model showed the same trend like *k-epsilon Realizable*; nevertheless, its resulting temperatures were lower.

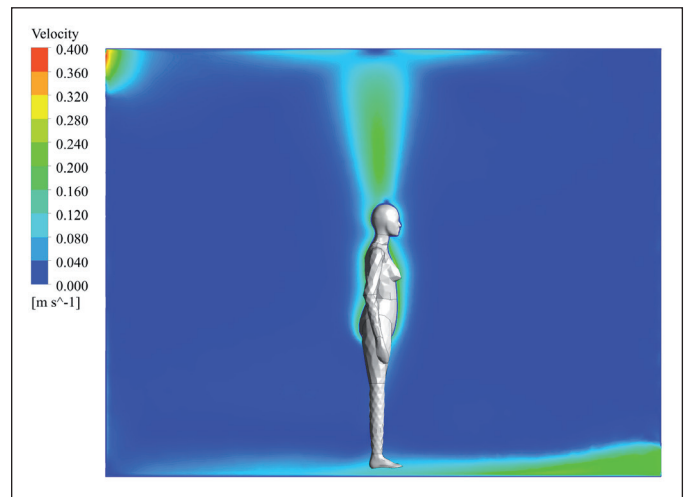


Fig. 13 Velocity contours along the symmetry plane

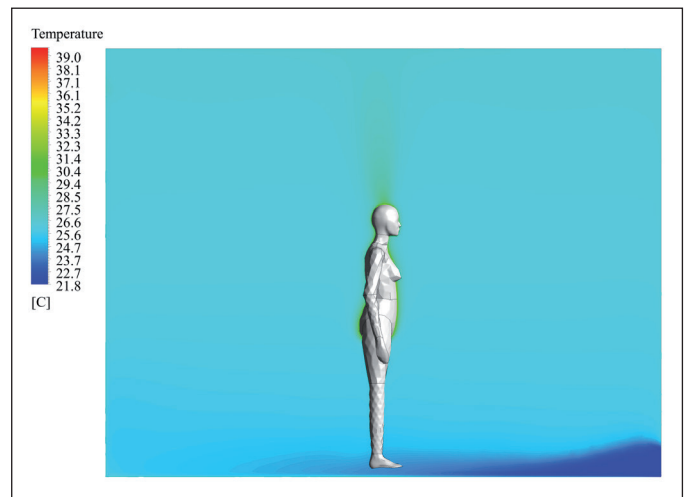


Fig. 14 Temperature contours along the symmetry plane

The lowest air temperatures were found in the case with the $k-\omega$ SST turbulence model. Yet, this model copied the trend of the velocity profile in L4 very well, where, in contrary, the $k-\varepsilon$ turbulence models overestimated the results. Both models ($k-\varepsilon$ Realizable and $k-\omega$ SST) are widespread in the field of indoor environment modelling.

This study is part of the ongoing research focused on the complex numerical modelling of a human body in an indoor environment. Another part of the research is the evaluation of the methods of heat transfer modelling between the human body and its surroundings (fixed surface temperature vs. fixed heat flux), the influence of radiation modelling, the ways of solving the heat transfer coefficients, etc. The result will be a verified virtual manikin that can be used for assessing the indoor environment whenever in-situ measurements are not feasible. Furthermore, it will be possible to extend the model by other functions such as a breathing model and to focus on the study of the issue of air pollutants spreading and the inhaled air quality. Currently, this can only be carried out using a thermal manikin together with, for example, PIV measurements, which is rather expensive and inflexible. In addition, the virtual environment allows one to change the boundary conditions practically without any limitations and to model very specific spaces.

Contact: lucie.dobiasova@fsv.cvut.cz

This paper was supported by SGS17/120/OHK1/2T/11.

Literature

- [1] *Guideline 10P: Interactions Affecting the Achievement of Acceptable Indoor Environments*, Second Public Review. Atlanta, USA: ASHRAE, 2010.
- [2] DE GIULI V., DA POS O., DE CARLI M. Indoor environmental quality and pupil perception in Italian primary schools. In: *Building Environment*, 2012, Vol. 56, pp. 335-345.
- [3] BLUYSSSEN P., FERNANDES E., FANGER P. O., GROES L., et al. *European Audit Project to Optimize Indoor Air Quality and Energy Consumption in Office Buildings* (No. LESO-PB-REPORT-2008-006), 1995.
- [4] FISK W. J., LEI-GOMEZ Q., MENDELL M. J. Meta-analyses of the associations of respiratory health effects with dampness and mold in homes. In: *Indoor Air*, 2007, Vol. 17, Issue 4, pp. 284-296.
- [5] WARGOCKI P., SUNDELL J., BISCHOF W., BRUNDRETT G., et al. Ventilation and health in nonindustrial indoor environments: report from a European multi-disciplinary scientific consensus meeting (EUROVEN). In: *Indoor Air*, 2002, Vol. 12, Issue 2, pp. 113-128.
- [6] BJORN E., NIELSEN P. V. Dispersal of Exhaled Air and Personal Exposure in Displacement Ventilated Rooms. In: *Indoor Air*, 2002, Vol. 12, No. 3, pp. 147-164.
- [7] Brohus H., Nielsen P. V. Personal exposure in ventilated rooms with concentration gradients. In: *Proceedings of Healthy Buildings 1994*, Vol. 2, pp. 559-564.
- [8] BJORN E., NIELSEN P. V. CFD simulation of contaminant transport between two breathing persons. In: *Proceedings of Roomvent 1998, The 6th International Conference on Air Distribution in Rooms*, Stockholm, Sweden, Vol. 1, pp. 133-140.
- [9] GAO N., NIU J. Transient CFD simulation of the respiration process and inter-person exposure assessment. In: *Building and Environment*, 2006, Vol. 41, pp. 1214-1222.
- [10] NIELSEN P. V., MURAKAMI S., KATO S., TOPP C., YANG J. H. *Benchmark Tests for a Computer Simulated Person*. Department of Building Technology and Structural Engineering Aalborg University, Denmark, ISSN 1395-7953 R0307, 2003.
- [11] Topp C., Hesselholt P., Trier M. R., Nielsen P. V. Influence of geometry of thermal manikins on contaminant distribution and personal exposure. In: *Proceedings of Healthy Buildings 2003*, Vol. 2, pp. 357-362.
- [12] BROHUS H. *Personal exposure to contaminant sources in ventilated rooms* [PhD thesis]. Denmark: Aalborg University, 1997.
- [13] DEEVY M., GOBEAU N. *CFD modelling of benchmark test cases for a flow around a computer simulated person*. HSL/2006/51. Buxton, UK: Health and Safety Laboratory, 2006.
- [14] SORENSEN D. N., VOIGT L. K. Modelling Flow and Heat Transfer around a Seated Human Body by Computational Fluid Dynamics. In: *Building and Environment*, 2003, Vol. 38, pp. 753-762.
- [15] RUSSO J., KHALIFA H. E. Computational study of breathing methods for inhalation exposure. In: *HVAC&R Research*, 2011, Vol. 17, Issue 4, pp. 419-431.
- [16] MURAKAMI S., ZENG J., HAYASHI T. CFD analysis of wind environment around a human body. In: *Journal of Wind Engineering and Industrial Aerodynamics*, 1999, Vol. 83, pp. 393-408.
- [17] NILSSON H. O., BROHUS H., NIELSEN P. V. CFD Modeling of Thermal Manikin Heat Loss in a Comfort Evaluation Benchmark Test. In: *Proceedings of Roomvent 2007, The 10th International Conference on Air Distribution in Buildings*, Helsinki, Finland, 2007.
- [18] HAYASHI T., ISHIZU Y., Kato S., MURAKAMI S. CFD analysis on characteristics of contaminated indoor air ventilation and its application in the evaluation of the effects of contaminant inhalation by a human occupant. In: *Building and Environment*, 2002, Vol. 37, pp. 219-230.
- [19] ITO K., INTHAVONG K., KURABUCHI T., UEDA T., et al. CFD Benchmark Tests for Indoor Environmental Problems: Part 3 – Numerical Thermal Manikins. In: *International Journal of Architectural Engineering Technology*, 2015, Vol. 2, pp. 50-75.
- [20] VILLI G., DE CARLI M. Detailing the effects of geometry approximation and grid simplification on the capability of a CFD model to address the benchmark test case for flow around a computer simulated person. In: *Building simulation*, 2014, Vol. 7, pp. 33-35.
- [21] SREBRIC J., VUKOVIC V., HE G., XANG X. CFD boundary conditions for contaminant dispersion, heat transfer and airflow simulations around human occupants in indoor environments. In: *Building and Environment*, 2008, Vol. 43, pp. 294-303.
- [22] DEEVY M., SINAI Y., EVERITT P., VOIGT L., GOBEAU N. Modelling the Effect of an Occupant on Displacement Ventilation with Computational Fluid Dynamics. In: *Energy and Buildings*, 2008, Vol. 40, pp. 255-264. ISSN 0378-7788.
- [23] TAGHINIA J. H., RAHMAN M. M., LU X. Effects of different CFD modeling approaches and simplification of shape on prediction of flow field around manikin. In: *Energy and Buildings*, 2018, Vol. 170, pp. 47-60.
- [23] HOMMA H., YAKIYAMA M. Examination of free convection around occupant's body caused by its metabolic heat. In: *ASHRAE Transaction*, 1988, Vol. 94, pp. 104-124.
- [24] VOELKER C., MAEMPEL S., KORNADT O. Measuring the human body's microclimate using a thermal manikin. In: *Indoor Air*, 2014, Vol. 24, pp. 567-579.